# Microcellular Injection Molded Polylactic Acid/Poly (ε-caprolactone) Blends With Supercritical $CO_2$: Correlation Between Rheological Properties and Their Foaming Behavior

**Haibin Zhao,[1] Xingru Yan,[2] Guoqun Zhao,[1] Zhanhu Guo[2]**
[1] *Key Laboratory for Liquid-Solid Structural Evolution and Processing of Materials (Ministry of Education), School of Materials Science and Engineering, Shandong University, Jinan, Shandong 250061, China*
[2] *Integrated Composites Laboratory (ICL), Department of Chemical and Bimolecular Engineering, University of Tennessee, Knoxville, Tennessee 37996*

**A systematic study on the rheological properties helps to identify suitable processing and compositional windows for foaming polylactic Acid (PLA)/poly ε-Caprolactone)(PCL) blends. In this article, the correlation between the rheological behavior, the blend morphology, as well as the resultant cellular structure of microcellular injection molded PLA/PCL blends was investigated. The addition of PCL had a significant effect on the storage modulus of PLA melts. With increasing the PCL content (less than 30%), the storage modulus increased due to the entanglement of polymer chains. The enhancement on their complex viscosities led to a better foaming behavior and pore microstructure. Porous structures with enhanced pore uniformity, decreased cell size, and higher cell density were observed in the PLA/PCL (70:30) specimens.** POLYM. ENG. SCI., 56:939–946, 2016.


## INTRODUCTION

Currently, more than 200 million tons of polymer are used for packaging applications annually. Of these, about 4 million tones are foamed polymers that are manufactured from synthetic polymers such as expanded polystyrene (EPS). Polymeric foams are lightweight structural materials with low density, high impact resistance, and also good insulation property. The main commercial interest for microcellular foams is based on the claim that mechanical properties would remain those of the base polymer, along with a significant density reduction [1, 2]. However, the main challenges for the current foamed packaging made from synthetic polymers are to recycle cost-effectively, and subsequently only a very small proportion is recycled, with the vast majority going to landfill [3]. As a consequence, the market place is looking for a solution to produce the foam packaging with biodegradable and environment-friendly polymer materials. Of the renewable polymers being commercialized, polylactic Acid (PLA) is produced in sufficient quantity to be a commercial solution. Thus, the technology for developing a new alternative foam packaging based on PLA has been widely studied by the researchers either from academic or industry [4, 5].

PLA is an aliphatic bio-based and biodegradable polyester. It has comparable mechanical performance to polyethylene terephthalate (PET) in terms of its tensile strength, elastic modulus, and barrier properties. However, the major obstacle for PLA foaming is its low melt strength and melt elasticity in stabilizing the foamed cell structure. Another drawback of PLA is its relatively poor thermal stability and narrow processing window, which lead to the chain-scission during the processing [6, 7]. Microcellular injection molding, known commercially as the MuCell® process, is capable of mass-producing parts with complex geometries and excellent dimensional stability, and is widely used in automotive, electronic/electrical products, and many other applications. In this process, supercritical fluid (SCF), usually nitrogen ($N_2$), or carbon dioxide ($CO_2$), is mixed with polymer melt to create a single-phase polymer/gas solution, which is then injected into the mold cavity, and finally the bubbles are formed in the product. The benefit of the technology is lower injection pressures, lower temperatures, shorter cycle time, less energy, and less material [8, 9]. By taking advantages of this technology, PLA can be foamed under a lower temperature to avoid its thermal degradation and produce semi-durable and durable products with complex geometries. However, the addition of supercritical fluid brings the complexity of flow and foaming behavior, which is much different from the conventional injection molding and limits its wide applications in industry. Thus, many studies have been conducted both on the modification of PLA (such as filler addition, copolymerization) and equipment upgrading (such as counter pressure, special screw design) [10–13]. But it seems like there is little room to develop the products with reliability, uniformity, and stability, which are important for industry applications and market.

Physical blending is believed as an economical and convenient route to create new materials with the desired combination of properties. A very wide range of properties can be achieved by this approach to meet the requirements of the targeted applications in relatively short time and at low cost compared to the developments of new monomers and polymerization techniques. Various bio-polymers such as polyglycolic acid (PGA), poly(lactide-*co*-glycolide) (PLGA), and polyhydroxybutyrate (PHB) blended with PLA have been investigated to tailor PLA's melt strength and to produce the microcellular foam with good cellular structure [14, 15]. Poly(ε-caprolactone) (PCL) is a commercially available aliphatic–aromatic copolyester with high ductility and good processability. Therefore, blending PLA with such synthetic biodegradable polymers could provide one way

*Correspondence to*: Z. Guo; e-mail: zguo10@utk.edu or G. Zhao; e-mail: gqzhao@sdu.edu.cn
Contract grant sponsor: National Natural Science Foundation of China; contract grant number: 51403118; contract grant sponsor: Distinguished Middle-Aged and Young Scientist Encourage and Reward Foundation of Shandong Province; contract grant number: BS2014ZZ010; contract grant sponsor: Fundamental Research Funds of Shandong University; contract grant numbers: 2014GN001 and 2014QY003-12.
DOI 10.1002/pen.24323
Published online in Wiley Online Library (wileyonlinelibrary.com).

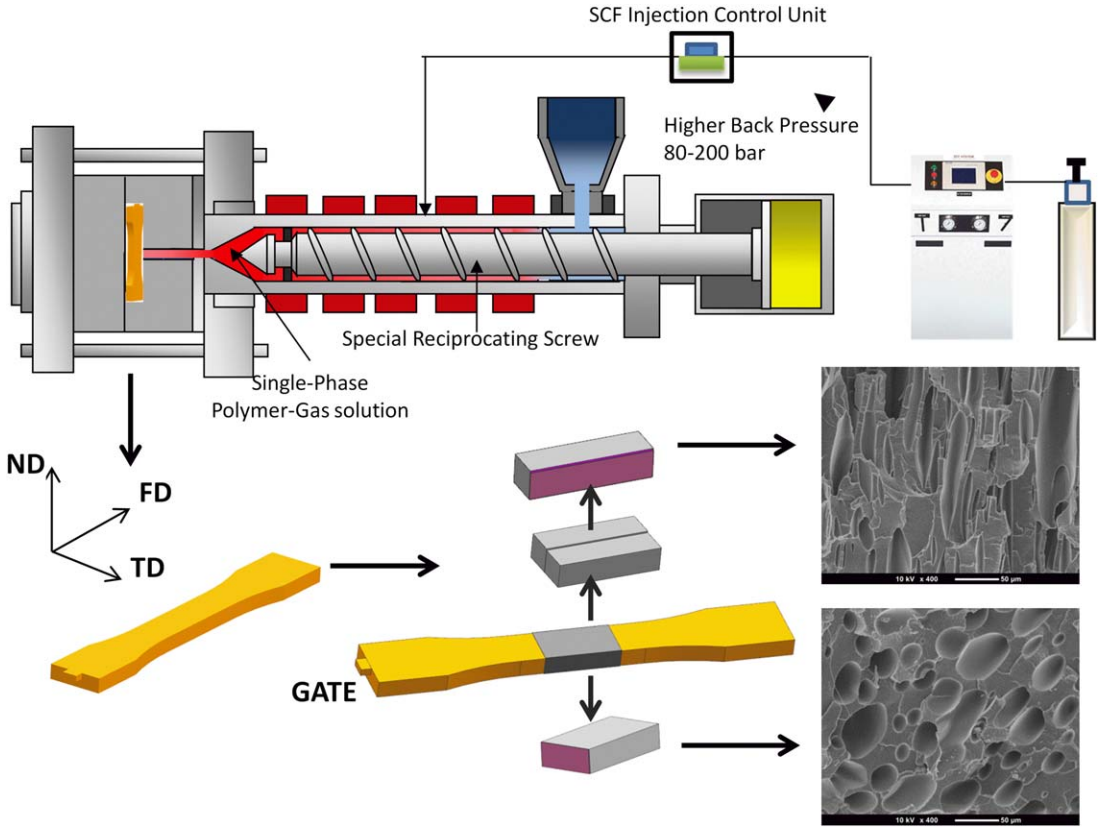


FIG. 1. Schematic diagrams of the microcellular injection molding with SCF and the standard dumbbell shape tensile bars: FD-the flow direction, TD-the transverse direction, and ND-the normal direction of "FD-TD" plane. [Color figure can be viewed in the online issue, which is available at wileyonlinelibrary.com.]

of achieving adequate ductility and processability without compromising biodegradability. However, based on the authors' knowledge, the study on the structure and properties of microcellular injection molded PLA/PCL blends has not been reported. Especially, the foaming behavior and their nucleation mechanism in the presence of the second phase PCL, as well as their changes in the rheological behavior, blends morphology, and interfacial effect have not been systematically studied. Moreover, the correlation between the rheological properties and the final cellular structure is not established yet.

The study on the rheological properties of PLA/PCL melts is crucial to gain fundamental understanding of the microcellular injection molding PLA/PCL blends with ideal cellular structure and properties. This article aims at illustrating how the addition of PCL impacts the melt rheology and foaming behavior of PLA. The linear and nonlinear shear rheological behaviors of PLA/PCL melts were studied using an ARES rheometer and correlated to the final foam morphology.

## EXPERIMENTAL

### *Materials*

Commercial PLA (4060D) was purchased from NatureWorks® LLC (Minnetonka, MN). Its specific gravity was 1.24 and its melt flow index was around 7.0 g/10 min (210°C/2.16 kg). Poly(ε-caprolactone) (CaPa 6500, $M_n = 50{,}000$) used in this study was a commercial product from Perstorp Polyols Inc, Toledo, OH. The melting point reported by the supplier was 58–60°C. Its MI was about 7.9 g/min (2.16 kg, 160°C). Both materials were used as received and in pellet form. All specimens were dried in an oven at 65°C overnight to remove any excess moisture.

### *Preparation of PLA/PCL Blends*

The PLA/PCL blends with mixture ratio of 90/10, 70/30, 50/50, and 30/70 wt% were compounded using a co-rotating twin-screw extruder with a screw diameter of 27 mm and an L/D ratio of 42. The extrusion temperature was independently controlled on eight zones along the extruder barrel and a strand die to achieve a temperature profile ranging from 165 to 180°C. The screw speed was maintained at 100 rpm for all the specimens. After compounding, the extruded melt strands were quenched in a water bath and subsequently pelletized. The reason to run pure resins, namely, PLA/PCL (100:0), through the twin-screw extruder was to ensure that all specimens undergo the same thermal-mechanical treatment and history.

### *Microcellular Injection Molding*

Standard tensile test bars (ASTM D638-03, Type I) were injection molded using an Arburg Allrounder 320S (Lossbrug, Germany) with a 25 mm diameter screw and equipped with microcellular injection molding capability (Trexel®, Inc., Wilmington, MA). The processing conditions for microcellular

 DOI 10.1002/pen

TABLE 1. Experimental conditions for microcellular injection molding processes.

| Supercritical fluid | | Molding conditions | |
|---|---|---|---|
| SCF flow rate (kg/h) | 1.1 | Nozzle temperature (°C) | 190 |
| SCF injection pressure (MPa) | 30 | Mold temperature (°C) | 10 |
| SCF dosage time (sec) | 1.7 | Injection speed ($cm^3$/s) | 20 |
| | | Cooling time (sec) | 60 |
| | | Back pressure (MPa) | 4 |

injection molding were listed in Table 1. Basically, there were four steps to create the foam products: (1) During plasticization, the precisely metered amounts of supercritical fluid (SCF), typically nitrogen or carbon dioxide, were introduced into the polymer through injectors mounted on the plasticizing barrel. (2) Homogeneous mixing of the supercritical fluid into the polymer through the special designed mixing section of the plasticizing barrel, creating a single phase solution of SCF and molten polymer. (3) Injection of polymer into mold cavities. The cells started to nucleate once exposed to lower pressure in the mold cavity. Molecular dispersion of SCF provided a homogeneous closed cell structure with a solid skin layer. (4) Low pressure filling of mold cavities. The pack/hold stage is absent in microcellular injection molding due to the homogeneous packing pressure that results from the nucleation and growth of micron scale cells. Figure 1 shows the schematic diagrams of the microcellular injection molding with SCF.

*Linear Rheological Properties*

The rheological behaviors of the PLA/PCL blends under oscillatory shear flow were investigated using a AR 2000 stress-controlled rheometer from TA Instruments, New Castle, DE. A parallel-plate geometry ($\phi = 25$ mm) with a fixed gap of 1 mm was selected for all the tests. The samples were cut from the microcellular injection molded bars in disks of 25 mm diameter. First, the strain sweep mode was performed to determine the limits of linear viscoelastic response of the melts. The value was used in both time sweep and frequency sweep modes later on to make sure all of the specimens were tested in the linear viscoelastic region (LVE).

The linear rheological measurements were performed by applying a time dependent strain of $\gamma(t)=\gamma_0\sin(\omega t)$ and measuring the resultant shear stress $G(t)=\gamma_0[G'(\omega)\sin(\omega t) + G''(\omega)\cos(\omega t)]$, where $G'(\omega)$ and $G''(\omega)$ are the storage and loss modulus, respectively. The frequency sweep was run from a high-to-low frequency mode at an angular frequencies range of 0.1 to 100 rad/s at a temperature of 190°C.

*Steady-State Shear Measurements*

The steady-state shear measurements at 190°C were also conducted to investigate the nonlinear rheological properties of the PLA/PCL melts. The shear rates ranging from 0.01 to 10 1/s were employed.

*Scanning Electron Microscopy*

The morphologies of the microcellular injection molded PLA/PCL blends were examined using a scanning electron microscope (SEM LEO 1530) with an accelerating voltage of

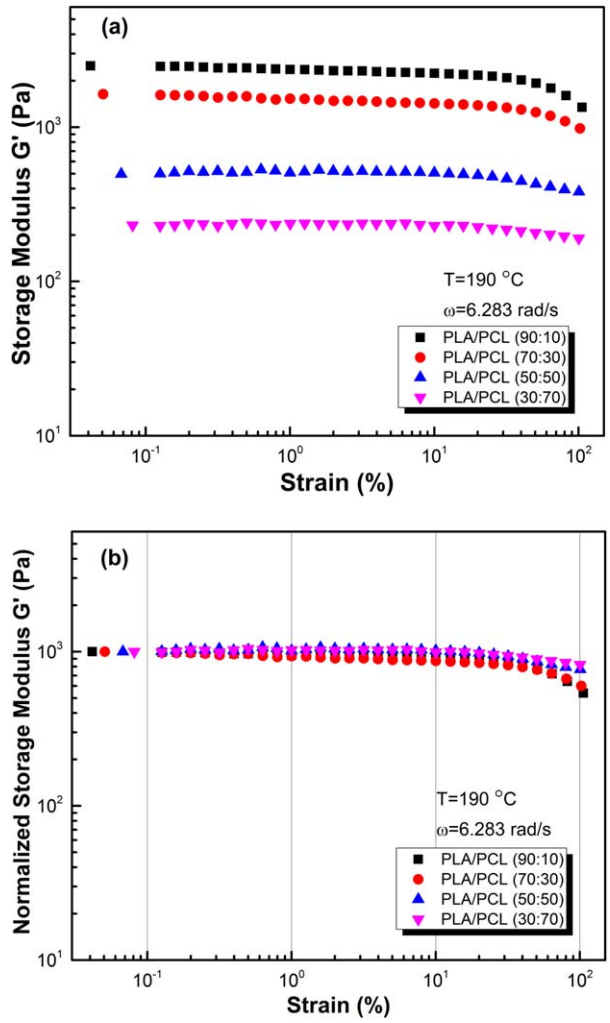


FIG. 2. Regular (a) and normalized (b) strain amplitude dependence of storage modulus at a constant frequency of 1 Hz at 190°C for PLA/PCL blends. [Color figure can be viewed in the online issue, which is available at wileyonlinelibrary.com.]

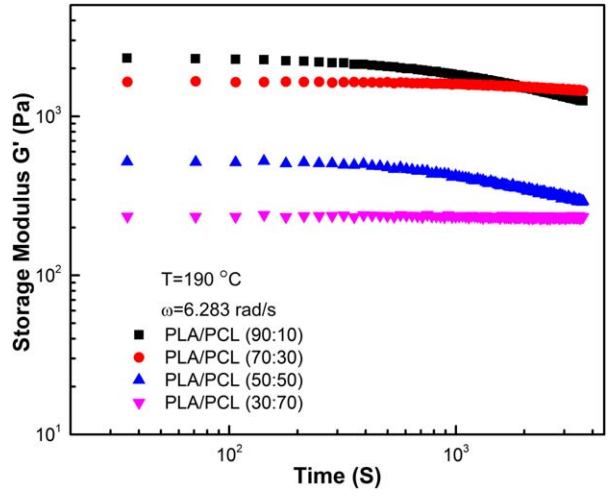


FIG. 3. Time sweep curves for PLA/PCL blends at 190°C. [Color figure can be viewed in the online issue, which is available at wileyonlinelibrary.com.]

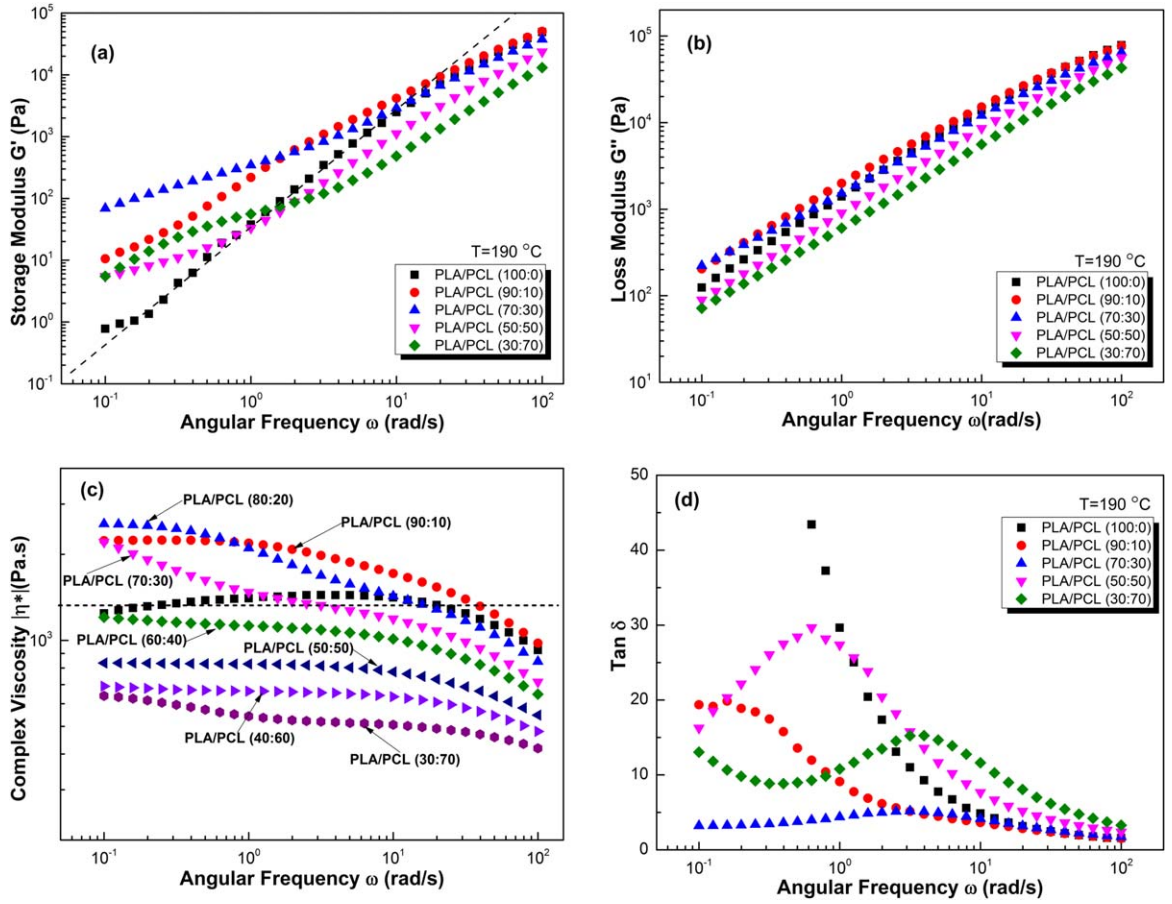


FIG. 4. Frequency dependence of (a) storage modulus and (b) loss modulus, (c) complex viscosity, and (d) tan $\delta$ of PLA/PCL blends with different compositions measured at 190°C. [Color figure can be viewed in the online issue, which is available at wileyonlinelibrary.com.]

5 kV. The SEM specimens were taken from the cross-section at the middle of the molded tensile bars, which were fractured in liquid nitrogen and then gold coated prior to observation for better imaging.

The cell size was analyzed using an image analysis tool (UTHSCSA Image Tool) and the cell density was calculated using *Eq. 1* [16]:

$$\text{Cell density} = \left(\frac{N}{L^2}\right)^{3/2} M \tag{1}$$

where $N$ is the number of cells, $L$ is the linear length of the area, and $M$ is a unit conversion resulting in the number of cell per $cm^3$. To be consistent, these data were obtained using the SEM micrographs taken from the center portion of the cross-section of the tensile bars.

## RESULTS AND DISCUSSION

*Oscillatory Shear and Linear Viscoelastic Properties*

During the microcellular injection molding process, after the single-phase polymer-gas molten injected into the mold cavity, the bubble nucleation and growth are actually occur at atmospheric pressure. Thus, the regular rheological measurements tested in the atmospheric environment could examine the effect of rheological properties on the microstructure of resultant microcellular samples.

**Strain Sweep Results.** To determine the linear viscoelastic limits of PLA/PCL melts, the dynamic strain sweep measurements were performed at 190°C and a frequency of 1 Hz. As shown in Fig. 2a, with increasing the PCL in the blends, the storage moduli of the melts decreased. But for each sample, the storage modulus could keep consistence with a high strain amplitude. To compare the transition of the curves, normalized strain amplitude dependence of storage modulus is shown in Fig. 2b. It can be seen that the linear viscoelastic limits extend to a strain as high as 30%, indicating that the PLA/PCL melts can keep a linear viscoelastic response at a wide range of strain. Therefore, the strain was set at 5% for time and frequency sweep to make sure the response of the PLA/PCL melts in a linear viscoelastic region.

**Time Sweep Results.** Figure 3 shows the time sweep results in the linear viscoelastic region for PLA/PCL blends. The PLA/PCL (90:10) and (50:50) blends exhibit a decreasing storage modulus as a function of time in half an hour, while the storage modulus of the PLA/PCL (70:30) and (30:70) specimens keeps a constant values for the whole range of test time sweep. With

 DOI 10.1002/pen

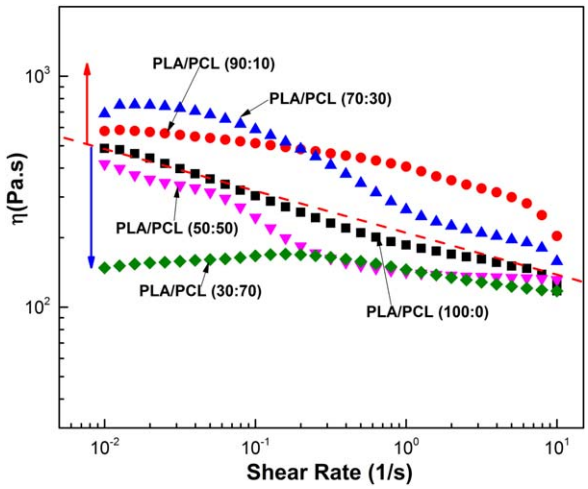


FIG. 5. Steady shear viscosity of PLA/PCL blends at 190°C. [Color figure can be viewed in the online issue, which is available at wileyonlinelibrary.com.]

increasing the PCL in the blends, the stability of the curves did not show a simple trendy either increasing or decreasing. Detailed frequency sweep study will be conducted in the following section to explore the reason for the complication of the storage modulus change. Thus, to avoid the thermal degradation of the specimens, the following frequency sweep was conducted in 22 min.

**Frequency Sweep Results.** The rheological properties of polymers have been identified as a key parameter to determine their foaming behavior. Dynamic shear measurements provide a detailed insight into the state of phase interactions in the polymer blend melts. The addition of another phase into the polymer matrix will significantly affect the rheological response of the blend system. It was reported that there is a percolation threshold with increasing the minor phase content that is reflected by the change of viscosity. Below the percolation threshold, the rheological behavior of the polymer matrix under shear is slightly affected by the dispersed phase due to the hydrodynamic forces. Once the minor phase content reached a critical value, the entanglement of polymer chains occurred due to the phase-phase interaction, and significant enhancement in storage modulus especially at low frequency would show up, which was related to a transition from the liquid to a pseudo-solid-like behavior [17, 18].

The viscoelastic behaviors of the polymer melts appeared as a combination of both irreversible viscous flow due to the polymer chain slippage and reversible elastic deformation due to molecular entanglement [19]. To compare the difference of rheological properties between neat PLA and PLA/PCL blends, frequency sweep for all of the samples was conducted. Figure 4 shows the frequency dependence of storage and loss modulus, complex viscosity, and tan δ of neat PLA and PLA/PCL blends with different compositions measured at 190°C.

As shown in Fig. 4a, compared to the curves of neat PLA, the addition of PCL had a significant effect on the storage modulus of PLA melts, especially in the low frequency region. A lower slope and high moduli indicate the formation of polymer chains entanglement in the PLA/PCL melts. The enhanced storage modulus suggests that the blends have a long relaxation time. At higher frequencies, the specimens experiencing a short thermal history exhibit an overlapping of the storage modulus curves. Similar to the results in time sweep, the enhancement of storage modulus at low frequency did not show a continuous increasing trendy. When the content of PCL was increased from 10 to 30%, their storage modulus was increased, while the curves of PLA/PCL (50:50) and (30:70) was moved back and closer to the curves of neat PLA. It is mainly because that the PCL chains have more movement ability than PLA at the testing temperature of 190°C. When the content of PCL was less than

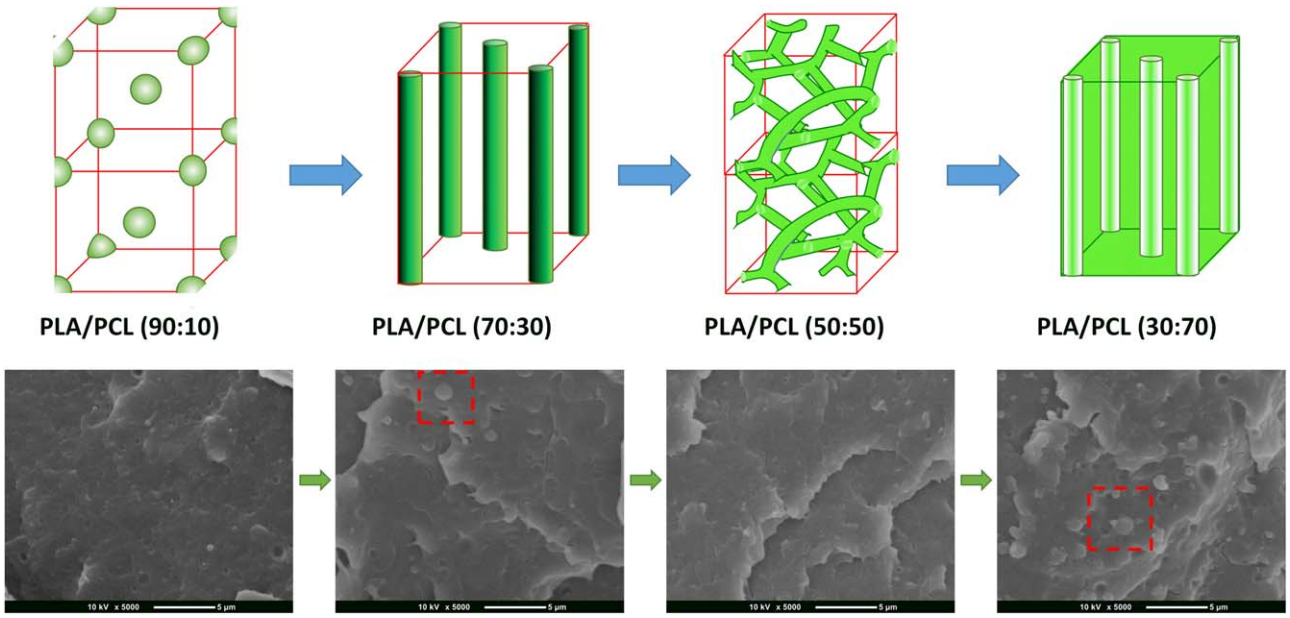


FIG. 6. Schematic diagrams of the morphological evolution and representative SEM micrographs of cryo-fractured surfaced of PLA/PCL blends. [Color figure can be viewed in the online issue, which is available at wileyonlinelibrary.com.]

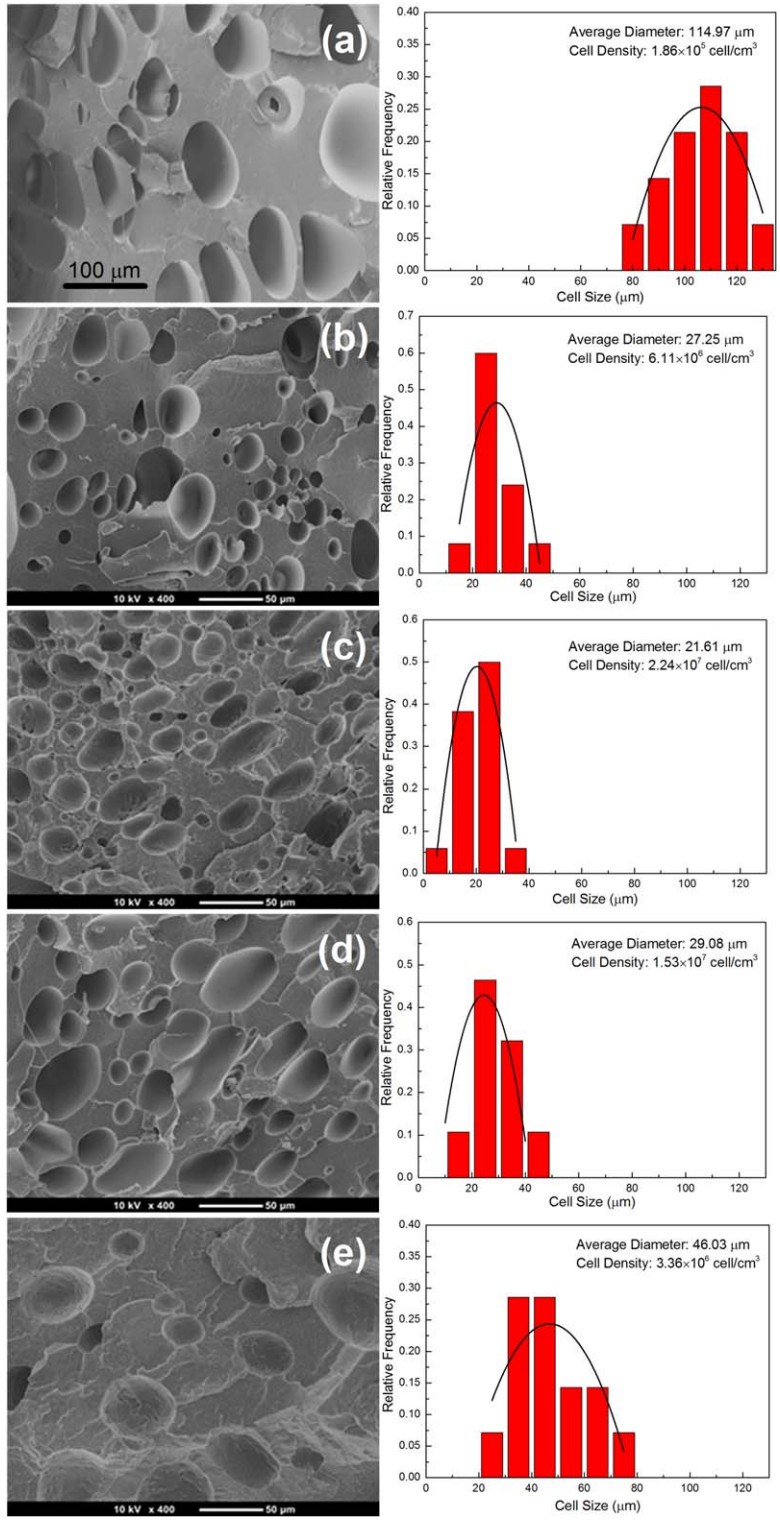


FIG. 7. Representative SEM micrographs of the cellular microstructures and corresponding cell size distribution plots for various microcellular injection molded PLA/PCL blends: (a) 100/0 wt%; (b) 90/10 wt%; (c) 70/30 wt%; (d) 50/50 wt%; and (e) 30/70 wt%. [Color figure can be viewed in the online issue, which is available at wileyonlinelibrary.com.]

50%, as a minor phase, the PCL chains were entangled with the PLA chains, leading to high reversible elastic deformation of the polymer melts. However, PCL turned to be the major phase with increasing the PCL content in the blend. The melting temperature of PCL was reported to be 60°C, thus, the relaxation of entangled polymer chains turned to be easier due to their high energy, and the entanglement density was decreased [20, 21]. Therefore, from Fig. 4a, the storage moduli of PLA/PCL

 DOI 10.1002/pen

(50:50) and (30:70) are observed to be lower than that of PLA/PCL (90:10) and (70:30) at the full range of frequency. Moreover, compared to neat PLA, the enhancement of storage modulus at low frequency was significant for the PLA/PCL (50:50) and (30:70) blends, while lower storage modulus than neat PLA was observed at the frequency higher than 1 rad/s.

The effect of PCL was less profound in the loss modulus than in the storage modulus (shown in Fig. 4b). With increasing the frequency, the curves of loss moduli of the blends with different composition showed a linear increase as well. All the curves paralleled with each other without any significant change. It was also noticed that the loss modulus of PLA/PCL (50:50) and (30:70) was still lower than that of neat PLA counterpart at the full range of frequency, indicating that the response of the specimens was mainly determined by the properties of the polymer blend matrices.

The curves of dynamic complex viscosity $\eta^*$ of neat PLA and PLA/PCL blends at 190°C as a function of angular frequency are shown in Fig. 4c. The complex viscosities $\eta^*$ of neat PLA melt kept a constant value in the whole range of testing frequency. The shear-thinning only appeared at the terminal of the curves, indicating that neat PLA displayed a Newton-liquid-like behavior. With the frequency increasing up to 10 rad/s, the shear thinning behavior was observed. To accurately examine the change of the complex viscosity, the frequency dependence of complex viscosity for the specimens with various compositions ranging from 90/10, 80/20, 70/30, 60/40, 50/50, 40/60, and 30/70 in weight ratio was shown. As expected, an increase of the PCL content led to higher shear viscosities. The zero shear viscosity of the PLA/PCL (90:10), (80:20), and (70:30) was higher than that of neat PLA. Especially for PLA/PCL (90:10), a significant enhancement of complex viscosity was observed as shown in Fig. 4c. However, when the amount of PCL was more than 40%, a general decreasing trend was observed. As for the shear-thinning tendency, there was no much difference for all the PLA/PCL melts with different compositions. With increasing the PCL content in the blends, the samples showed a similar shear-thinning tendency.

Figure 4d shows the loss factor, tan $\delta$, as a function of frequency for all the specimens. The tan δ is the ratio between the loss modulus and the storage modulus. In general, the tan $\delta$ peak shifted toward a higher frequency with increasing the PCL content. The improvement of the complex viscosity for PLA/PCL (90:10), (80:20), and (70:30) specimens was expected to have a positive effect on their foaming process and structure. Further investigation will be conducted in the following part of morphology section.

*Steady Shear and Nonlinear Viscoelastic Properties*

The steady shear rheological behaviors of neat PLA and PLA/PCL melts are shown in Fig. 5. Both neat PLA and PLA/PCL melts behaved as typical non-Newtonian fluids. Profound shear-thinning phenomenon was observed for almost all the specimens under investigation except PLA/PCL (30:70). At lower shear rates, the shear viscosities of PLA/PCL (90:10) and (70:30) melts are higher than that of neat PLA melt. For the PLA/PCL (70:30) specimen, the shear-thinning tendency became much stronger so that the shear viscosities of PLA/PCL (70:30) melts were even equal to that of neat PLA melt at high shear rates. Compared to PLA/PCL (90:10), with increasing the PCL content in the blends, the PLA/PCL (70:30) showed a more profound shear-thinning tendency. The enhancement is ascribed to the chain stretching of PCL in the blend via trapped entanglements between PLA and PCL. For PLA/PCL (50:50) and (30:70), in which PLA as the minor phase, their steady shear viscosities were lower than neat PLA at the set testing temperature. Moreover, PLA/PCL (30:70) behaved as Newtonian-liquid like behavior without obvious shear-thinning. The enhanced rheological properties for the blend system is important from the viewpoint of microcellular injection molding applications, in which the elongation flow takes place dominantly during foaming.

*Morphology and Microstructure of PLA/PCL Blends*

To investigate the phase morphology of the PLA/PCL blends, the fractured surfaces were observed by SEM after being gold coated. Figure 6 shows the schematic diagrams of the morphological evolution and representative SEM micrographs of cryo-fractured surfaces of the PLA/PCL blends containing 10%, 30%, 50%, and 70%wt PCL dispersed in PLA, and their immiscible nature is clearly evident. PLA/PCL (90:10) and (70:30) shows a well dispersed PCL phase domains, which are in spherical shape in the PLA matrix. The average size of PCL region increased with increasing the PCL fractions from 10 to 30 wt%. With increasing the PCL fraction to 50 wt%, the transitions from a immiscible particle morphology to a co-continuous two-phase morphology were observed in the PLA/PCL (50:50) specimen. Further increasing the PCL content to 70 wt%, a two-phase immiscible structure with PLA regions appearing as clearly defined spheres is shown on the fractured surfaces of PCL matrix phase. The phase morphology of PLA and PCL blend was also studied by Wu et al., they concluded that these two polymers were immiscible in the whole composition range [22, 23]. Park et al. [24] studied the foam PCL/PLA blend by using the solid-liquid phase separation method and subsequent freeze-drying method. The DSC results showed that the immiscibility of PCL and PLA caused the phase separation morphology. Thus, the macroscopic mechanical properties and the microscopic deformation behavior were affected by the phase separation. Aslan et al. [25] prepared the PLA/PCL membranes to study their microstructure by using random copolymer poly(lactide-*co*-caprolaction). The dispersed phase was found to be spherically distributed in the other phase, indicating their immiscibility.

The porous morphologies of the microcellular injection molded PLA/PCL blends and the cell size distribution of the foams are presented in Fig. 7. To analyze the effect of PCL on the foaming behavior of PLA, the SEM micrograph of neat PLA produced at the same processing condition is presented in Fig. 7 for comparison. As shown in Fig. 7a, neat PLA shows a board distribution on the fractured surface with big cells as large as 90 μm, and a low cell density. With the addition of 10 and 30 wt% PCL in the blends, porous morphology with enhanced pore uniformity and higher cell density was observed. It can be seen in Fig. 7b and c, the average cell size is decreased and the cell density is increased with increasing the weight ratio of PCL. The cell nucleation in the final microcellular injection molded specimen was significantly affected by the dispersion of minor phase and the overall morphology of the blends. The addition of small amounts of PCL increased the cell density, indicating a heterogeneous nucleation effect of the PCL phase [9, 26].

According to the classical nucleation theory, the minor phase and their interfaces in a multiphase system serve as heterogeneous nucleation sites and lower the surface free energy by decreasing the intermolecular potential energy of polymer [27, 28]. For an immiscible blend system, the addition of a second-phase component reduces the activation energy barrier for bubble nucleation because of the large amount of interfacial volume in the blends [29]. Thus, with the addition of PCL and increasing the interface area in the PLA/PCL blends, the surface energy decreased and resulted in a reduction of heterogeneous nucleation energy and an increase of nucleation density. Due to the low energy barrier, supercritical fluid is easy to dissolve in the polymer matrix. However, a continuously increase of the PCL content does not lead to a higher cell density. For PLA/PCL (50:50) specimen, cell coalescence occurred and some of irregular pores are observed in Fig. 7d, which are attributed to their lower viscosity and melt strength. In particular, there are some large cells shown up, demonstrating that some cells burst and coalesce together. Normally, pore coalescence occurs when the energy distribution in the blend system is uneven during pore growth [30]. In general, to reach a stable equilibrium state, smaller pores tend to merge into bigger pores to obtain the lowest energy [10]. For a multiphase and multicomponent system, different gas diffusion/solubility in individual component and the accumulation tendency of SCF at the interface between two phases lead to a nonuniform gas distribution in the polymer blend system. The results indicate that the final pore structure of the polymer blends is related not only to the phase structure of the blends but also to their melt strength.

From Fig. 7e, only several big pores with uneven sizes were found in the porous morphology of the PLA/PCL (30:70) specimens, indicating low gas concentration and solubility in the polymer melts. The gas diffusion is crucial to the development of final porous morphology. Due to the low melt strength, the polymer melt is hard to restrict gas diffusion until the growth of the pore. As a result, a maximum in the cell density was only found at 30 wt% PCL for PLA/PCL blend system. The foaming behavior and final pore structure may be influenced by the combination of many factors, such as the nature of second-phase component, potential intermolecular interaction on polymer blends, phase structure of the blends, and their rheological properties.

## CONCLUSIONS

A detailed and systematic evaluation of the rheological properties of PLA/PCL blends over a wide composition range was carried out. The effect of the rheological properties and blend morphology on the final cellular structure of microcellular injection molded PLA/PCL blends was investigated. The addition of PCL was found to have a significant effect on the storage modulus of PLA melts. With increasing the PCL content (less than 30%), the storage modulus was increased due to the entanglement of polymer chains. The enhancement on their complex viscosities lead to a better foaming behavior and pore microstructure. Porous morphology with enhanced pore uniformity, decreased cell size, and higher cell density was observed in PLA/PCL (70:30) specimens, as the heterogeneous nucleation effect of PCL and enhanced rheological properties of the blend system.

## REFERENCES


1. X. Chen, M.C. Heuzey, and P.J. Carreau, *Polym. Eng. Sci.*, **44**, 2158 (2004).
2. H. Zhao and G. Zhao, *J. Mech. Behav. Biomed. Mater.*, **53**, 59 (2016).
3. J.W. Rhim, H.M. Park, and C.S. Ha, *Prog. Polym. Sci.*, **38**, 1629 (2013).
4. K.M. Nampoothiri, N.R. Nair, and R.P. John, *Bioresour. Technol.*, **101**, 8493 (2010).
5. R. Auras, B. Harte, and S. Selke, *Macromol. Biosci.*, **4**, 835 (2004).
6. M. Nofar and C.B. Park, *Prog. Polym. Sci.*, **39**, 1721 (2014).
7. R.E. Drumright, P.R. Gruber, and D.E. Henton, *Adv. Mater.*, **12**, 1841 (2000).
8. H.B. Zhao, Z.X. Cui, X.F. Wang, L.S. Turng, and X.F. Peng, *Compos. Part B Eng.*, **51**, 79 (2013).
9. H. Zhao, Z. Cui, X. Sun, L.S. Turng, and X. Peng, *Ind. Eng. Chem. Res.*, **52**, 2569 (2013).
10. H. Zhao, X. Peng, B. Chen, and N. Li, *Polym. Plast. Technol. Eng.*, **54**, 822 (2015).
11. M. Mihai, M.A. Huneault, and B.D. Favis, *Polym. Eng. Sci.*, **50**, 629 (2010).
12. Y.W. Di, S. Iannace, E. Di Maio, and L. Nicolais, *Macromol. Mater. Eng.*, **290**, 1083 (2005).
13. M.J. Yuan, A. Winardi, S.Q. Gong, and L.S. Turng, *Polym. Eng. Sci.*, **45**, 773 (2005).
14. L.T. Lim, R. Auras, and M. Rubino, *Prog. Polym. Sci.*, **33**, 820 (2008).
15. S. Pilla, A. Kramschuster, L.Q. Yang, J. Lee, S.Q. Gong, and L.S. Turng, *Mat. Sci. Eng. C-Bio. S*, **29**, 1258 (2009).
16. M.J. Yuan and L.S. Turng, *Polymer*, **46**, 7273 (2005).
17. J.K. Kim and H.W. Son, *Polymer*, **40**, 6789 (1999).
18. A. Ajji, L. Choplin, and R.E. Prud'homme, *J. Polym. Sci. Part B (Polym. Phys.)*, **26**, 2279 (1988).
19. Q. Fang and M.A. Hanna, *Ind. Crop. Prod.*, **10**, 47 (1999).
20. P. Spitael and C.W. Macosko, *Polym. Eng. Sci.*, **44**, 2090 (2004).
21. D.H.S. Ramkumar and M. Bhattacharya, *Polym. Eng. Sci.*, **38**, 1426 (1998).
22. D. Wu, Y. Zhang, M. Zhang, and W. Zhou, *Eur. Polym. J.*, **44**, 2171 (2008).
23. Y. Zhang, D. Wu, M. Zhang, W. Zhou, and C. Xu, *Polym. Eng. Sci.*, **49**, 2293 (2009).
24. J.E. Park and M. Todo, *J. Mater. Sci.*, **46**, 7850 (2011).
25. S. Aslan, L. Calandrelli, P. Laurienzo, M. Malinconico, and C. Migliaresi, *J. Mater. Sci.*, **35**, 1615 (2000).
26. H. Zhao, G. Zhao, L.S. Turng, and X. Peng, *Ind. Eng. Chem. Res.*, **54**, 7122 (2015).
27. A.M. Harris and E.C. Lee, *J. Appl. Polym. Sci.*, **107**, 2246 (2008).
28. Y.M. Corre, A. Maazouz, J. Duchet, and J. Reignier, *J. Supercrit. Fluid*, **58**, 177 (2011).
29. M. Yamaguchi and K.I. Suzuki, *J. Polym. Sci. Part B: Polym. Phys.*, **39**, 2159 (2001).
30. X. Liao, H. Zhang, Y. Wang, L. Wu, and G. Li, *RSC Adv.*, **4**, 45109 (2014).